Spectrochimica Acta Part A: Molecular and Biomolecular Spectroscopy 262 (2021) 120099

Contents lists available at ScienceDirect

Spectrochimica Acta Part A: Molecular and Biomolecular Spectroscopy

journal homepage: www.elsevier.com/locate/saa

A rhodamine based chemosensor for solvent dependent chromogenic sensing of cobalt (II) and copper (II) ions with good selectivity and sensitivity: Synthesis, filter paper test strip, DFT calculations and cytotoxicity

Wei Chuen Chan [a], Hazwani Mat Saad [b], Kae Shin Sim [b], Vannajan Sanghiran Lee [a], Chee Wei Ang [c], Keng Yoon Yeong [c], Kong Wai Tan [a,*]

[a] *Department of Chemistry, Faculty of Science, Universiti Malaya, 50603 Kuala Lumpur, Malaysia*
[b] *Institute of Biological Sciences, Faculty of Science, Universiti Malaya, 50603 Kuala Lumpur, Malaysia*
[c] *School of Science, Monash University Malaysia Campus, Jalan Lagoon Selatan, Bandar Sunway, Selangor 47500, Malaysia*

HIGHLIGHTS

- A new rhodamine based chemosensor **1** was synthesized and characterized.
- Selectively detect Co^{2+}/Cu^{2+} in different solvent systems (MeCN and DMF).
- Sensor **1** as copper (II) ion detector can be reused with proper treatment.
- Filter paper test strip for detection of Co^{2+} and Cu^{2+} in pure aqueous solution.
- Sensor **1** showed no significant cytotoxicity towards CCD-18Co and HT-29 cell lines.

GRAPHICAL ABSTRACT

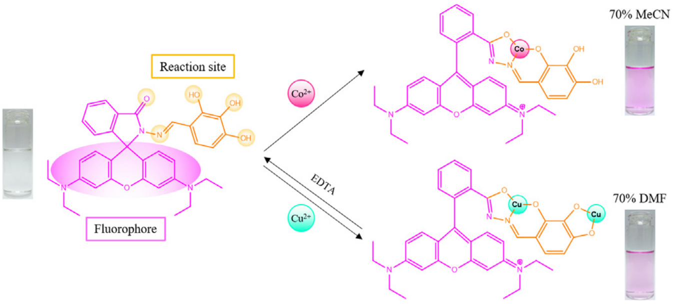

ARTICLE INFO

Article history:
Received 20 March 2021
Received in revised form 9 June 2021
Accepted 19 June 2021
Available online 23 June 2021

Keywords:
Chemosensor
Rhodamine
"Naked-eye" detection
Solvent dependent sensing
Co^{2+}
Cu^{2+}

ABSTRACT

A new chemosensor **1** was synthesized by reacting rhodamine B hydrazide and 2,3,4-trihydroxybenzaldehyde, which was then characterized by spectroscopic techniques and single crystal X-ray crystallography. Sensor **1** has the ability to sense Co^{2+}/Cu^{2+} ions by "naked-eye" with an apparent colour change from colourless to pink in different solvent system, MeCN and DMF respectively. Furthermore, it can selectively detect Co^{2+}/Cu^{2+} among wide range of different metal ions, and it exhibits low detection limit of 4.425×10^{-8} M and 1.398×10^{-7} M respectively. Binding mode of the two complexes were determined to be 1:1 stoichiometry for Co^{2+} complex and 1:2 stoichiometry for Cu^{2+} complex through Job's plot, IR spectroscopy, mass spectrometry and ^1H NMR spectroscopy. Moreover, reversibility of the sensor **1** as copper (II) ion detector was determined by using EDTA and the results showed that sensor **1** can be reused for at least 6 cycles. Other than that, a low cost chemosensor test strips were fabricated for the convenient "naked-eye" detection of Co^{2+} and Cu^{2+} in pure aqueous media. The MTT assay was conducted in order to determine the cytotoxicity of sensor **1** towards human cell lines.

1. Introduction

Essential trace elements such as metal ions play an important role in biological system and are fundamental to the health of living

---

* Corresponding author.
E-mail address: kongwai@um.edu.my (K.W. Tan).

https://doi.org/10.1016/j.saa.2021.120099
1386-1425/

organisms. Trace elements such as cobalt, copper, iron, zinc and others are needed to mediate vital biochemical reactions and human body requires about 100 mg per day to stay healthy [1]. However, overload of these elements in the human body might cause several diseases, such as Alzheimer's and Parkinson's disease [2].

Cobalt is an essential trace element that is found in cobalamin [3]. Cobalamin is important in the formation of myelin, which is an insulating layer around the nerves [4]. Other than that, as an important component of vitamin B_{12}, cobalt plays major part in various biological system [5]. Studies showed that cobalt is not only important for human but also for plants, where the Co containing porphyrin enzyme can catalyses decarbonylation of aldehydes [6]. However, excess level of cobalt in human body could be dangerous and leads to various complications such as asthma, cardiac disease, lung disease and dermatitis [7]. Similar to cobalt, copper is also an essential trace element and is the third most abundant metal in human body [8]. Deficiency of copper in human body can cause several brain related diseases such as Alzheimer, Parkinson and Menkes disorder [9–12]. However, excess of copper is harmful to human body since copper is able to produce reactive oxygen species (ROS) that will obstruct cellular metabolism [13].

Hence, it is important to trace these metal ions in the surrounding in order to maintain good human health. Traditional quantitative approaches was able to detect these analytes at high accuracy using instruments such as atomic absorption spectrometry (AAS) and inductively coupled plasma atomic emission spectrometry (ICP-AES) [14,15]. However these methods have some disadvantages such as the need for sophisticated instrumentations, tedious sample preparation and trained operators. Hence, a chemosensor that allowed "naked eye" detection was preferred over these methods [16].

Synthesis of probe as Co^{2+} and Cu^{2+} detector have gained considerable interest from researchers, and much effort had been undertaken for developing fluorometric method [17–19]. However, fluorometric method is harder for real time detection due to the paramagnetic properties of Co^{2+} and Cu^{2+} that culminate to fluorescence quenching problem [20,21]. Compared to fluorometric probe, colorimetric detectors have obtained some interest for enabling "naked-eye" detection in a cheap and straightforward manner [22,23].

As a new design concept, chemosensors that can detect more than one metal ion are more favourable because it offer advantages such as cost reduction when comparing to a probe that can detect only one metal ion [24]. Multiple ions detection can be achieved by different methods such as combining multiple responsive units into one single probe, detection of metal ions using different mechanism, covalent approaches and others [24,25]. However, some of these methods require intense synthesis work. Furthermore, some of the reported sensor showed that the detectable change from different analytes that emerge at same time with same trend may cause some qualification error [26]. To overcome this issue, some had suggested "solvent dependent sensing" method [27,28]. Detection of multiple metal ions can be attained by using different reaction media which was done by Wang's group [27]. In that study, the acylhydrazide isoquinoline Schiff base sensor was able to detect Mg^{2+} in acetonitrile and Zn^{2+} in DMF-water.

Herein we presented a new rhodamine B Schiff base derivative based on a 2,3,4-trihydroxybenzaldehyde moiety, known as sensor **1**. The three hydroxyl group of the moiety might provide extra binding sites for metal ions, and it could help to improve the water solubility as well. Sensor **1** was able to sense Co^{2+} and Cu^{2+} in different solvent system with good sensitivity and selectivity. Other than that, detection of Co^{2+} and Cu^{2+} in pure aqueous media can be achieved by using the filter paper test strip fabricated. Furthermore, MTT assay was conducted to test the potential of sensor **1** for the detection of metal ions in living cells.

2. Experimental

2.1. Materials and instruments

Chemical reactants and solvents used for this research were bought from SIGMA and MERCK. Chloride salts and nitrate salts were used to prepare the 12 metal ions solution (Ag^+, Al^{3+}, Ca^{2+}, Cd^{2+}, Co^{2+}, Cu^{2+}, La^{3+}, Mn^{2+}, Na^+, Ni^{2+}, Pb^{2+}, Zn^{2+}). JEOL ECX spectrometer was used to obtain NMR spectra, with tetramethylsilane as internal reference and deuterated DMSO as solvent. FT-IR spectra were obtained on a Perkin-Elmer Spectrum RX-1 spectrometer. Shimadzu UV-2600 series spectrophotometer was utilized for absorption spectra. Mass spectra were recorded with a Waters Xevo TQ-S micro triple quadrupole mass spectrometer system using positive ESI.

2.2. Synthesis of rhodamine B hydrazide

Rhodamine B (0.479 g, 1 mmol) was dissolved in ethanol (20 mL) and hydrazine hydrate (0.5 mL) was added in excess. The solution was refluxed for 4 h until the colour of solution changes from dark purple to light orange. Then, the solution was cooled down and evaporated at room temperature. 1 M hydrochloric acid solution was added until a clear red solution was obtained, followed by addition of 1 M sodium hydroxide solution with slow stirring until pH 9–10 was achieved and a pink precipitate was formed. The precipitate formed was filtered and washed with distilled water. Lastly, recrystallization process was carried out using ethanol and purple crystals were obtained. Yield: (0.424 g, 92.9%). FT-IR (ATR, cm^{-1}): ν = 3332, 3246, 2962, 2925, 2866, 1716, 1687, 1633, 1613, 1373, 1215, 1116, 1017, 815, 753. ^1H NMR (400 MHz, DMSO d_6), δ (ppm): 1.06 (t, J = 7.2 Hz, 12H, NCH_2CH_3); 3.29 (q, J = 7.2 Hz, 8H, NCH_2CH_3); 4.25 (s, 2H, NH_2); 6.32 (s, 4H, Xanthene-H); 6.35 (d, J = 5.2 Hz, 2H, Xanthene-H); 6.95 (m, 1H, Aromatic-H); 7.46 (m, 2H, Aromatic-H); 7.77 (m, 1H, Aromatic-H). ^{13}C NMR (100 MHz, DMSO d_6), δ (ppm): 12.93 (NCH_2CH_3); 44.21 (NCH_2CH_3); 65.40 (C-N); 97.91, 105.76, 108.33, 122.76, 123.95, 128.17, 128.71, 128.94, 133.03, 148.68, 152.40, 153.54 (Aromatic-C); 166.01 (C=O).

2.3. Synthesis of sensor **1**, 3′,6′-bis(diethylamino)-2-((2,3,4-trihydroxybenzylidene)amino) spiro[isoindoline-1,9′-xanthen]-3-one

Rhodamine B hydrazide (0.0913 g, 0.2 mmol) and 2,3,4-trihydroxybenzaldehyde (0.0308 g, 0.2 mmol) was dissolved in ethanol and refluxed for 6 h as illustrated in Scheme 1. The reaction solution was concentrated and left to cool at room temperature. Upon slow evaporation of solvent, purple crystal was obtained and the resulting precipitate was filtered and washed with cold ethanol. Yield: (0.1023 g, 88.7%). FT-IR (ATR, cm^{-1}): ν = 3211, 2973, 2931, 1676, 1607, 1372, 1219, 1119, 1021, 813, 783. ^1H NMR (400 MHz, DMSO d_6), δ (ppm): 1.05 (t, J = 7.2 Hz, 12H, NCH_2CH_3); 3.29 (q, J = 6.8 Hz, NCH_2CH_3); 6.32 (m, 2H, Xanthene-H); 6.36 (d, J = 2.4 Hz, 1H, Aromatic-H); 6.42 (m, 4H, Xanthene-H); 6.56 (d, J = 8.8 Hz, 1H, Aromatic-H); 7.06 (d, J = 7.2 Hz, 1H, Aromatic-H); 7.57 (m, 2H, Aromatic-H); 7.88 (dd, J_1 = 2 Hz, J_2 = 1.2 Hz, 1H, Aromatic H); 8.39 (s, 1H, Imine-H); 8.93 (s, 1H, Hydroxyl-H); 9.63 (s, 1H, Hydroxyl-H); 10.59 (s, 1H, Hydroxyl-H). ^{13}C NMR (100 MHz, DMSO d_6), δ (ppm): 12.89 (NCH_2CH_3); 44.17 (NCH_2CH_3); 65.91 (C-N); 97.76, 105.09, 108.33, 108.69, 111.28, 122.44, 123.47, 124.21, 128.22, 129.15, 129.31, 129.39, 133.10, 134.31, 147.89, 149.05, 149.78, 151.63, 153.16 (aromatic C); 154.38 (C=N); 163.84 (C=O). ESI-MS m/z calc. for $C_{35}H_{36}N_4O_5$ [**1**+H]$^+$ 593.27, found 593.22. The structure of sensor **1** was further established by X-ray crystallography (Fig. 1). CCDC: 2080271. Crystal data

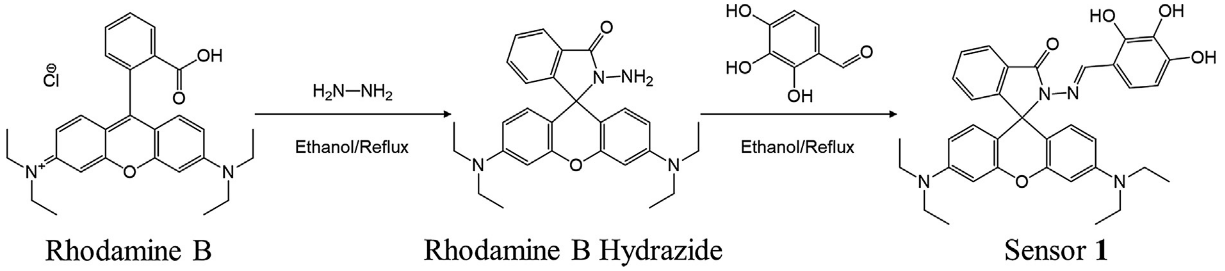

Scheme 1. Synthesis routes of sensor **1**.

shows that sensor **1** has a monoclinic crystal system with the space group of $P2_1/c$. As shown in Fig. 1, the xanthene and spirolactam moiety are forming a vertical plane that perpendicular to each other. These will break the conjugation of whole structure, explaining why free sensor **1** appears to be non-fluorescence in closed ring state.

2.4. Procedures of the metal ion sensing

Stock solution of sensor **1** (5 mM) was prepared in DMSO. On the other hand, nitrate salts and chloride salts of the 12 metal ions (Ag^+, Al^{3+}, Ca^{2+}, Cd^{2+}, Co^{2+}, Cu^{2+}, La^{3+}, Mn^{2+}, Na^+, Ni^{2+}, Pb^{2+}, Zn^{2+}) (5 mM) were prepared separately in distilled water. Sensor stock solution (3 μL) was placed in scintillation vial, diluted to 3 mL and added with an appropriate aliquot of each ion stock to obtain a test solution.

2.5. X-ray data

Oxford Rigaku SuperNova Dual diffractometer equipped with a Mo-Kα X-ray source (λ = 0.71073 Å) with Atlas detector was used to analyse the intensity data of the crystals and the unit cell parameters. Cell refinement, data acquisition and reduction were carried out with CrysAlis Pro software [29]. SADABS was used to carry out absorption corrections. The structure solution and refinements were done by using SHELXL97 [30]. Olex2 and Ortep3 was used to draw molecular graphics [31–33].

2.6. MTT cytotoxicity assay

The CCD18-Co (normal colon fibroblast) and HT-29 (human colorectal adenocarcinoma) cell lines used in this study were purchased from American Type Culture Collection (ATCC, USA). The MTT assay was carried out using the method previously described by Heng et al. [34] with cisplatin as positive control. The data was shown as mean ± standard deviation of triplicate experiments.

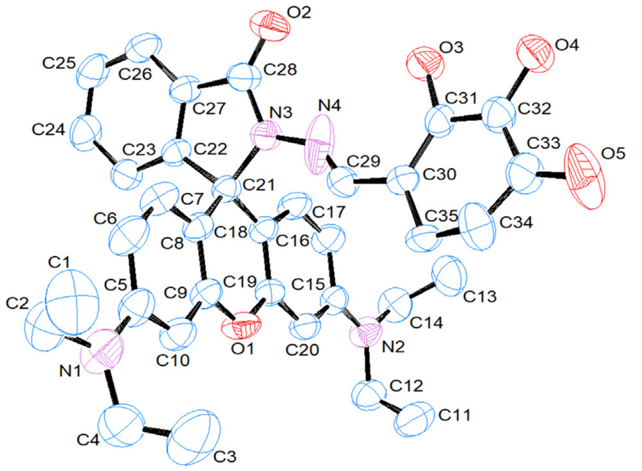

Fig. 1. ORTEP plot of sensor **1**. Hydrogen atoms were omitted for clarity. (Probability level = 50%).

3. Results and discussion

3.1. UV–Vis spectral response of sensor 1

To investigate the Co^{2+}/Cu^{2+} detection properties of sensor **1**, UV–Vis absorption response experiment was performed. The free sensor **1** was colourless with almost no absorption value above 560 nm, showing that rhodamine B spirolactam form was predominant. As shown in Fig. 2, upon addition of 1 equiv. of Co^{2+}/Cu^{2+} to the colourless solution of free sensor **1** (5 μM), the solution turned pink and showed a new absorption band at 558 nm in two different solvent systems, which are MeCN/HEPES buffer (7:3, v/v, pH 7.0) and DMF/HEPES buffer (7:3, v/v, pH 7.0) respectively. This suggested the formation of an open ring amide form upon complexation of sensor **1** with Co^{2+}/Cu^{2+}. Absorption spectra of sensor **1** in the presence of other metal ions such as Ag^+, Al^{3+}, Ca^{2+}, Cd^{2+}, Co^{2+}/Cu^{2+}, La^{3+}, Mn^{2+}, Na^+, Ni^{2+}, Pb^{2+} and Zn^{2+} were recorded to confirm the response of sensor towards various metal ions. The results showed that the other metal ions did not cause any new band formation and the sensor solution remain colourless. These observations demonstrate the potential of sensor **1** as a ‘naked-eye’ detector for Co^{2+}/Cu^{2+} ions.

3.2. Optimization of reaction condition

As shown in Fig. S1, sensor **1** in aq. DMSO did not show any noticeable response when Ag^+, Al^{3+}, Ca^{2+}, Cd^{2+}, La^{3+}, Mn^{2+}, Na^+, Ni^{2+}, Pb^{2+} and Zn^{2+} were added. However, the colour of solution changes from colourless to purple when Co^{2+} and Cu^{2+} were added. The colour change suggested that sensor **1** can be served as a potential candidate as a “naked-eye” detector of Co^{2+} and Cu^{2+}. Since both Co^{2+} and Cu^{2+} were showing similar colour changes, responsive signal that appear at the same time may cause qualification error. “Solvent-dependent sensing” method was used to overcome this problem. To optimize the reaction condition, choice of organic solvent, overall solvent-buffer composition, pH and reaction time were investigated.

3.2.1. Choice of organic solvent

Since sensor **1** was insoluble in pure aqueous solution, five organic solvent (ethanol, methanol, acetonitrile, DMSO and DMF) were chosen as co-solvent in the reaction media. However, free sensor **1** appeared as pink colour in aq. ethanol and aq. methanol solution as shown in Fig. S2. Such characteristic makes ethanol and methanol not suitable for the “naked-eye” “off-on” detection of metal ions. In aq. DMSO, sensor **1** was colourless and it turns purple in the presence of Co^{2+} and Cu^{2+}, the responsive signal that

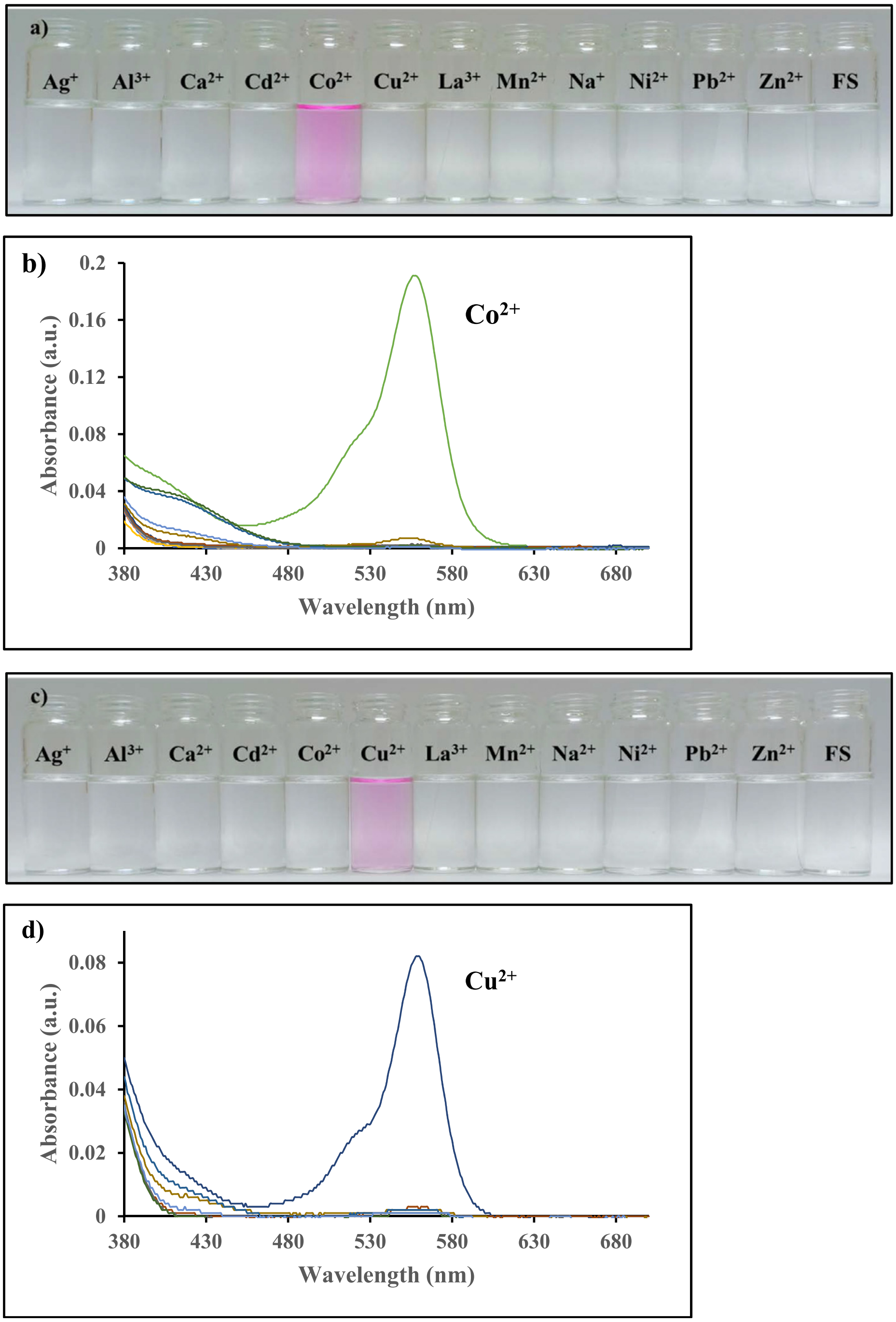

Fig. 2. a) Colour change and b) UV–Vis spectrum of sensor **1** (5 μM) with different metal ions (5 μM) in MeCN/HEPES buffer (7:3, v/v, pH7), 10 min incubation time. c) Colour change and d) UV–Vis spectrum of sensor **1** (5 μM) with different metal ions (5 μM) in DMF/HEPES buffer (7:3, v/v, pH7), 2 min incubation time.

appear at the same time may cause some qualification error. In aq. acetonitrile and aq. DMF, sensor **1** was able to selectively detect Co^{2+} and Cu^{2+} respectively by fine tuning the composition of organic and aqueous content.

3.2.2. Effect of aqueous content

As shown in Fig. S3, sensor **1** showed response towards Co^{2+} when 10% MeCN to 90% MeCN was used and the response towards Cu^{2+} began to show when there was 40% aqueous content in the reaction media (60% MeCN). Hence 70% MeCN was chosen as reaction media for the detection of Co^{2+}. On the other hand, sensor **1** showed response towards Cu^{2+} from 10% DMF to 90% DMF and the response towards Co^{2+} started to show when there was 40% aqueous content in the reaction media (60% DMF). Hence 70% DMF was chosen as reaction media for the detection of Cu^{2+}.

3.2.3. Effect of pH

To study the effect of pH and determine an appropriate pH range in which sensor **1** can detect Co^{2+}/Cu^{2+} effectively, acid base titration experiment was performed. As shown in Fig. S4, free sensor **1** did not show obvious characteristic colour change between pH 4.0–12.0, suggesting that the spirolactam ring remain closed and sensor **1** was insensitive towards pH change in this range. Addition of Co^{2+} causing the absorbance enhancement at pH range of 6.0–10.0, which is due to the opening of the spirolactam ring into ring open amide form. Besides, addition of Cu^{2+} led to the absorbance enhancement at pH range of 4.0–8.0. Result shows that sensor **1** may be used for the detection of Co^{2+}/Cu^{2+} in approximate physiological conditions. Therefore, further colorimetric assays were carried out in pH 7.0 HEPES buffered solution.

3.2.4. Effect of reaction time

The kinetic characteristics of the reaction system were studied and shown in Fig. S5. The absorbance value of free sensor **1** (5 μM) was almost zero and no obvious change was detected throughout the whole study, indicating that the spirolactam ring structure of sensor **1** is quite stable. Addition of Co^{2+} causes enhancement in the absorbance value and the value increased with reaction time. The absorbance value reached its maximum value at around 10th minutes. Hence, 10 min incubation time was chosen for the detection of Co^{2+} to ensure that the reaction between sensor **1** and Co^{2+} is complete. On the other hand, the interaction of sensor **1** with Cu^{2+} was completed within 2 min. So, 2 min incubation time was chosen for the detection of Cu^{2+}. Rapid response of sensor **1** allows this system to be used as real time monitoring of Co^{2+}/Cu^{2+}.

Thus, optimized reaction conditions for Co^{2+} and Cu^{2+} were 10 min incubation time in MeCN/HEPES buffer (7:3, v/v, pH 7), and 2 min incubation time in DMF/HEPES buffer (7:3, v/v, pH 7).

3.3. Various concentration of metal ions

To gain insight on the quantitative properties of sensor **1** towards Co^{2+}/Cu^{2+}, titration experiment was carried out with gradual addition of Co^{2+}/Cu^{2+} to the free sensor **1** solution. In different reaction system, the UV–Vis spectra of free sensor **1** were similar. As shown in Fig. 3b, free sensor **1** itself showing two absorption band at ~277 nm and ~324 nm, which may be due to π–π* and n–π* electronic transition [27]. Conjugation between the lone pair of imine group nitrogen atom and the π bond of the benzene ring may led to n–π* transition [35]. Upon gradual addition of Co^{2+}/Cu^{2+} to the free sensor **1**, new absorption band at 558 nm was observed and the absorbance value increased with the increasing concentration of metal ions. The presence of two isosbestic points at ~300 nm and ~353 nm indicate that the interaction between sensor **1** and Co^{2+}/Cu^{2+} were clean and no side reactions occurred [27].

Plots of absorbance value vs. concentration of metal ion were plotted in Fig. 3 inset. A good linear relationship between absor-

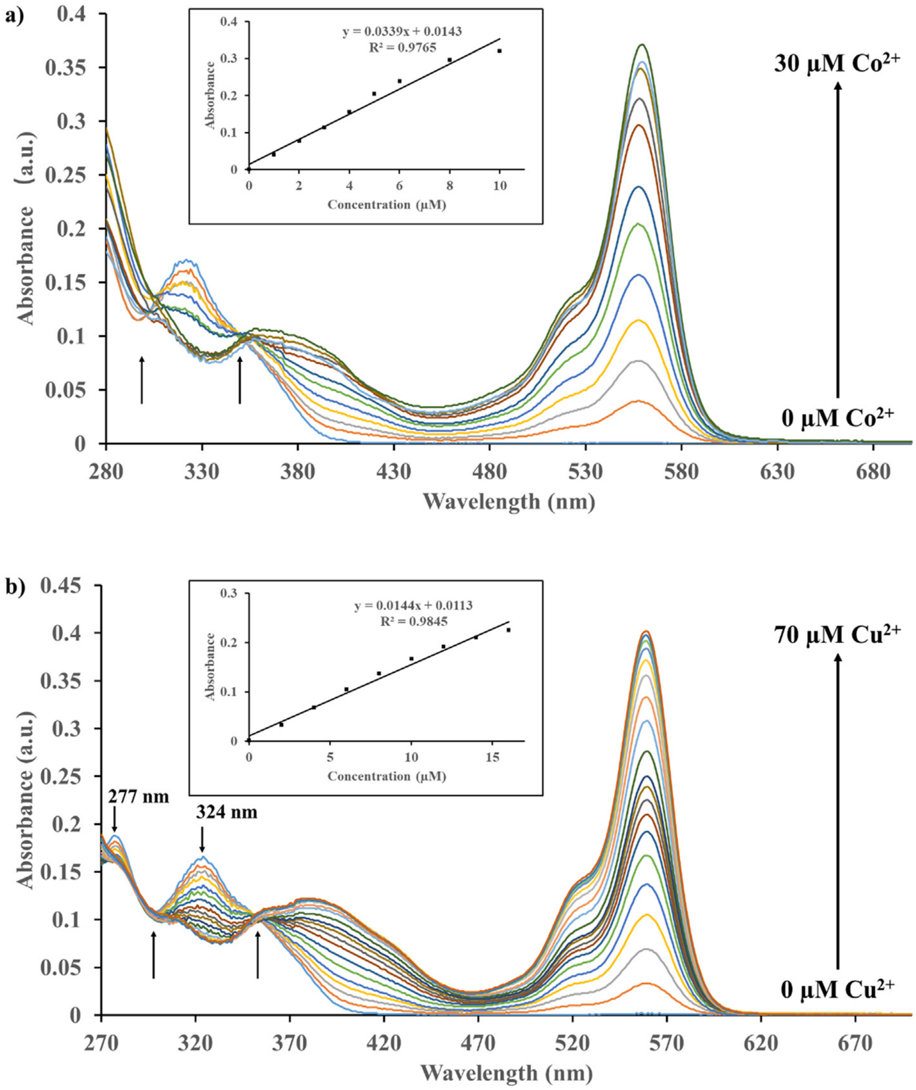

Fig. 3. Absorption spectra of sensor **1** (5 μM) with the increasing concentration of a) Co^{2+} in MeCN/HEPES buffer (7:3, v/v, pH 7) and b) Cu^{2+} in DMF/HEPES buffer (7:3, v/v, pH 7). Inset: Plot of absorbance value at λ_{max} 558 nm vs. concentration. [Sensor **1**] = 5 μM.

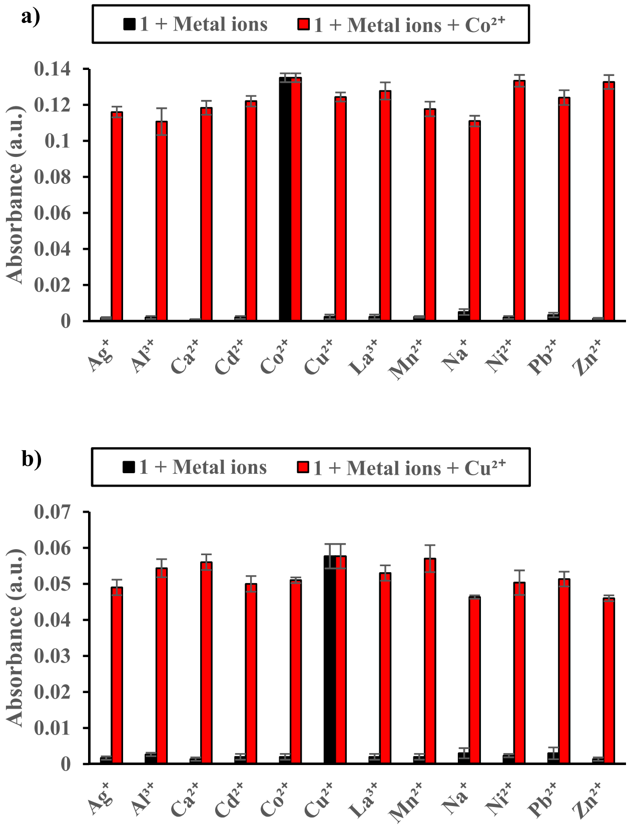

Fig. 4. UV–Vis absorbance response of sensor **1** (5 μM) at λ_{max} 558 nm to various cation in a) MeCN/HEPES buffer (7:3, v/v, pH 7) and b) DMF/HEPES buffer (7:3, v/v, pH 7). The black bars represent the absorbance of sensor **1** in the presence of cations of interest. The red bars represented changes that occur upon subsequent addition of a) Co^{2+} and b) Cu^{2+}. Data is expressed as mean ± SD (n = 3).

bance value and concentration of Co^{2+}/Cu^{2+} was observed in the range of 0–10 μM ($R^2 = 0.98$) and 0–16 μM ($R^2 = 0.98$) respectively. This showing the potential of sensor **1** to be use for the quantitative determination of cobalt (II) and copper (II) ion. Detection limit (LOD) of sensor **1** for Co^{2+}/Cu^{2+} were calculated using the equation LOD = 3 S_b/m, where S_b is the standard deviation of blank solution and m is the slope of calibration curve [36]. LOD for Co^{2+}/Cu^{2+} were calculated to be 4.42×10^{-8} M and 1.40×10^{-7} M, respectively.

The association constant, Ka of **1**-Co^{2+} and **1**-Cu^{2+} complexes were determined by the Benesi-Hildebrand equation [37]:

$$\frac{1}{A - A_0} = \frac{1}{A_{max} - A_0} + \frac{1}{A_{max} - A_0 K_a [M^+]}$$

where, A is the absorbance at the given concentration of metal ion, A_{max} is the absorbance at the maximum concentration of metal ion, and A_0 is the absorbance of the free sensor without metal ion. Association constant was studied graphically by plotting 1/A-A_0 vs. 1/[M^+]. Data were linearly fitted as shown in Fig. S7, and the Ka values were obtained using the slope and intercept of the graph. The Ka values of **1**-Co^{2+}/**1**-Cu^{2+} are 6.46×10^3 M^{-1} and 1.88×10^3 M^{-1}, respectively. High association constant, Ka indicates the high affinity of free sensor **1** towards Co^{2+}/Cu^{2+} ions [38].

*3.4. Tolerance of sensor **1** to Co^{2+}/Cu^{2+} over other metal ions*

The effects of other metal ions were evaluated through competitive experiment. The absorbance changes of sensor **1** were obtained after treatment of 1 equiv. of Co^{2+} in the presence of 1 equiv. other interfering metal ions, including Ag^+, Al^{3+}, Ca^{2+}, Cd^{2+}, Cu^{2+}, La^{3+}, Mn^{2+}, Na^+, Ni^{2+}, Pb^{2+} and Zn^{2+}. Similar procedure was repeated by replacing Co^{2+} with Cu^{2+}. As shown in Fig. 4, when sensor **1** acted as a cobalt (II) ion colorimetric probe, most of the metal ions barely perturbed the absorbance change of sensor **1** with Co^{2+}. The most inhibition of absorbance change was done by Al^{3+}, which was only 18% inhibition of the original absorbance of sensor **1** with Co^{2+}. When sensor **1** acted as a copper (II) ion colorimetric probe, Ni^{2+} and Zn^{2+} showed the most inhibition (20%) in the absorbance change of sensor **1** with Cu^{2+}. The interference of other metal ions was tabulated in Table S1. This observation confirms that sensor **1** is very selective towards Co^{2+} or Cu^{2+} even in the presence of other metal ions. Such characteristic is very important as the environment water sample usually contains mixture of ions.

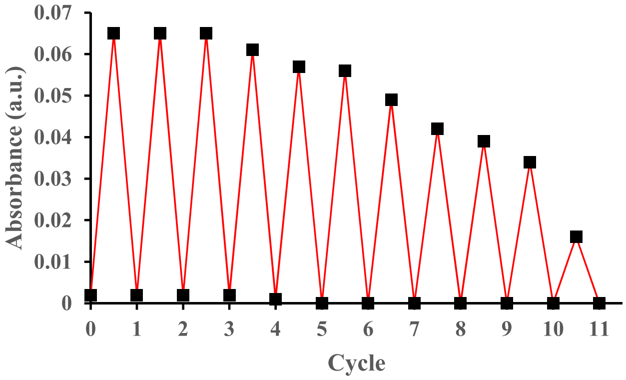

Fig. 5. UV–Vis absorbance response of sensor **1** (5 μM) at λ_{max} 558 nm after the sequential addition of Cu^{2+} (5 μM) and EDTA (5 μM) in DMF/HEPES buffer (7:3, v/v, pH 7).

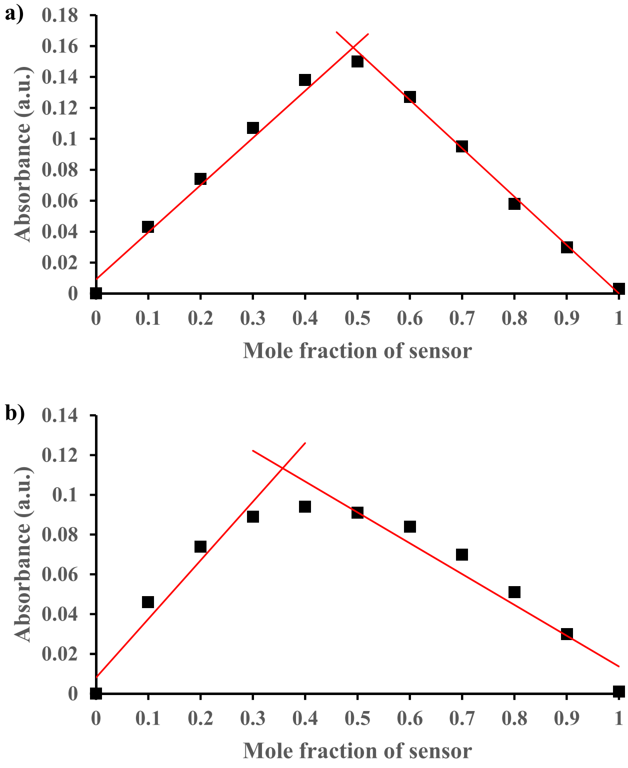

Fig. 6. Job's plot of complexes a) **1**-Co^{2+} in MeCN/HEPES buffer (7:3, v/v, pH 7) and b) **1**-Cu^{2+} in DMF/HEPES buffer (7:3, v/v, pH 7).

*3.5. Reversibility of the interaction between sensor **1** and Co^{2+}/Cu^{2+}*

Practical application of a sensor is much dependent on the reusability. The coordination between sensor **1** and Cu^{2+} was reversible, which was proven by adding EDTA into the solution containing sensor **1** and Cu^{2+}. As shown in Fig. 5, introduction of EDTA (5 μM) could immediately restores the absorbance of free sensor **1** (5 μM). When Cu^{2+} (5 μM) was added to the reaction solution again, the absorbance of sensor **1** was enhanced. This process could be repeated for 6 cycles before the absorbance value drops drastically. This shows that sensor **1** could be reused with proper treatment for the detection of Cu^{2+}. Besides, this also further supports that the colour change of colourless to pink is due to the complexation of **1**-Cu^{2+}.

While for Co^{2+}, interaction between sensor **1** and Co^{2+} will not be affected by EDTA. Addition of EDTA into the solution containing sensor **1** and Co^{2+} did not affect the absorbance spectrum as shown in Fig. S8. The absorbance value only decreased 9.4% even after addition of 1000 equiv EDTA.

*3.6. Binding mode of sensor **1** with Co^{2+}/Cu^{2+}*

Job's plot analysis was carried out to identify the binding stoichiometry between sensor **1** and Co^{2+}/Cu^{2+}, as shown in Fig. 6. For **1**-Co^{2+}, the maximum absorbance was observed when the mole fraction of sensor is around 0.5. This shows that the binding mode of the **1**-Co^{2+} is most likely a 1:1 binding stoichiometry. Whereas for **1**-Cu^{2+}, the maximum absorbance was observed when the mole fraction of sensor is around 0.33. Such observation shows that the formation of complex was the highest when the mole fraction of sensor is 0.33 and mole fraction of metal ions is 0.67, which is ratio of 1:2 with excess metal ions. Hence, the binding mode of **1**-Cu^{2+} is most likely a 1:2 (sensor: metal) binding stoichiometry.

IR spectra of sensor **1**, **1**-Co^{2+} and **1**-Cu^{2+} were obtained to study the binding mechanism (Fig. S9). For free sensor **1**, five bands at 3211 cm^{-1}, 1677 cm^{-1}, 1607 cm^{-1}, 1373 cm^{-1} and 1119 cm^{-1}, were ascribed to the OH hydroxyl, C=N imine, N-C=O amide carbonyl and C-N group respectively. Upon addition of Co^{2+}/Cu^{2+}, imine and amide carbonyl peak at 1677 cm^{-1} and 1607 cm^{-1}

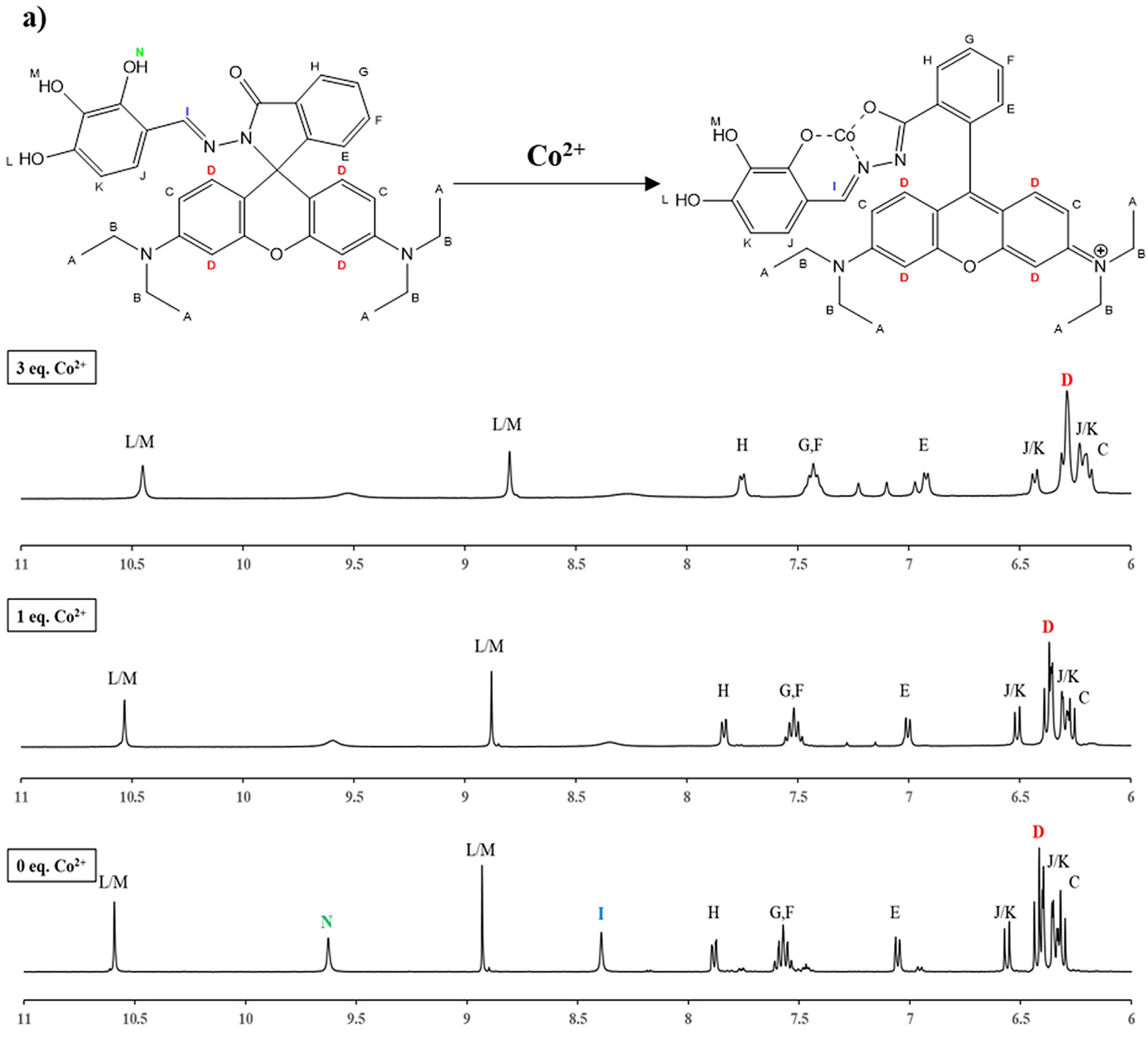

Fig. 7. ^1H NMR spectrum of sensor **1** in the presence and absence of a) Co^{2+} and b) Cu^{2+} in DMSO d_6.

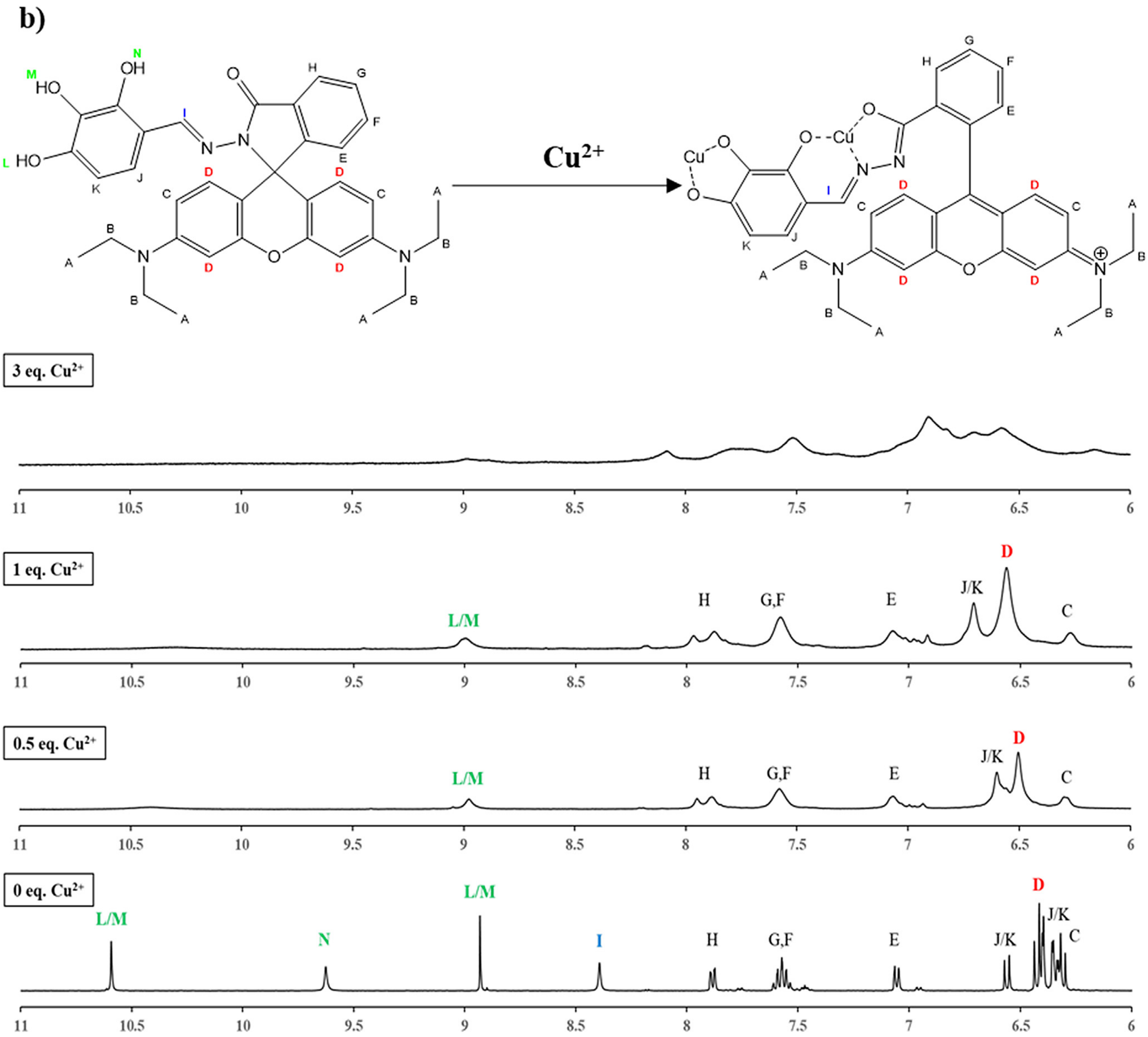

Fig. 7 (*continued*)

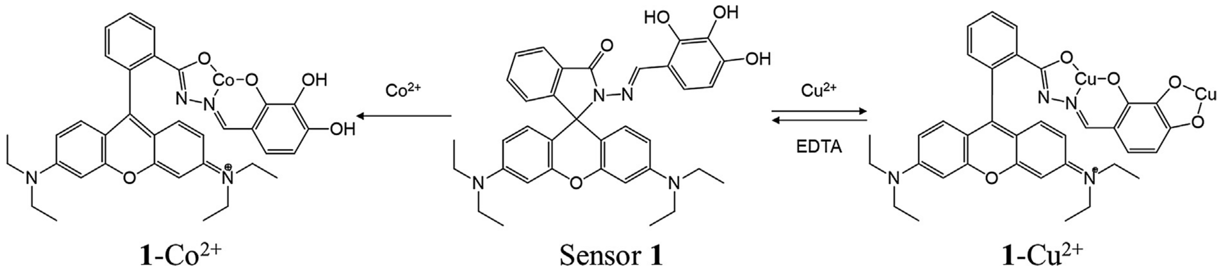

Scheme 2. Proposed mechanism for interaction between sensor **1** and Co^{2+}/Cu^{2+}.

shifted to 1643 cm^{-1} and 1583 cm^{-1} for **1**-Co^{2+}. While for **1**-Cu^{2+}, the two peaks shifted to 1647 cm^{-1} and 1586 cm^{-1}. These suggest that the imine N and amide carbonyl O of sensor **1** are involved in the coordination with Co^{2+}/Cu^{2+}. Opening of the spirolactam ring upon coordination with Co^{2+}/Cu^{2+} is proven by the disappearance of C-N peak at 1373 cm^{-1} and 1119 cm^{-1}. Binding stoichiometry of **1**-Co^{2+} was found to be 1:1 from previous Job's analysis. This was further supported by the IR spectrum of **1**-Co^{2+} since there was free OH peak in the spectrum, indicating that not all OH group are involved in coordination with Co^{2+}. While for **1**-Cu^{2+} which binds in 1:2 stoichiometry, disappearance of OH peak indicates that all the OH group were involved in coordination with Cu^{2+}.

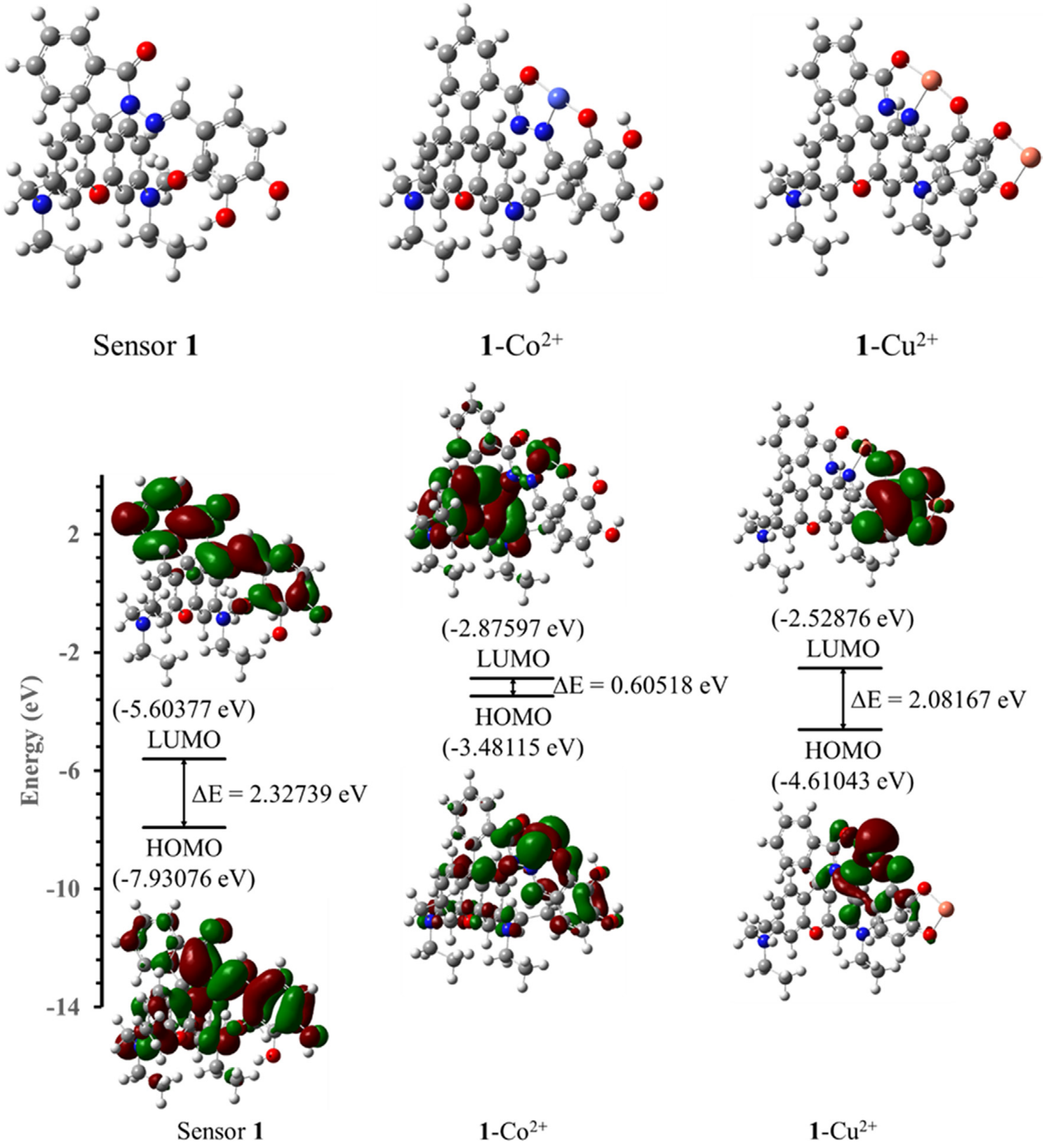

Fig. 8. Optimized structure of sensor **1**, **1**-Co^{2+}, **1**-Cu^{2+} calculated at B3LYP level using LANL2DZ basis set. Energy diagram of HOMO and LUMO of sensor **1**, **1**-Co^{2+}, **1**-Cu^{2+} calculated at B3LYP level using LANL2DZ basis set.

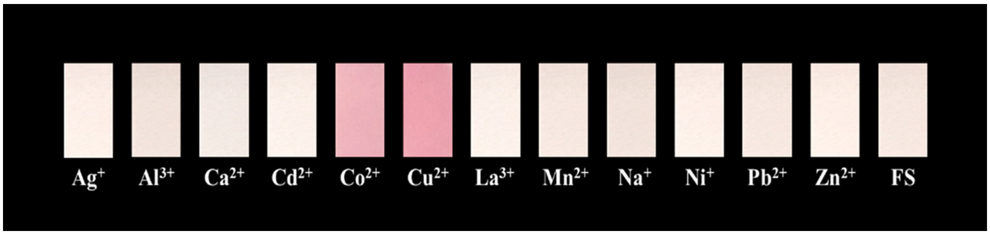

Fig. 9. Filter paper test strips of sensor **1** (5 mM) for the detection of different metal ions (100 μM) in 100% aqueous solution (water).

Interaction between sensor **1** and Co^{2+}/Cu^{2+} were further studied through ^1H NMR experiment in DMSO d_6. As shown in Fig. 7, peaks at 6.42 ppm were assigned to the proton signal of xanthene (H_D) and a downfield shift was observed upon addition of Cu^{2+} which indicates the formation of delocalized xanthene (upfield shift upon addition of Co^{2+}). Other than that, singlet peak at 8.39 ppm was assigned to proton signal of imine (H_I) and the proton signal disappeared after addition of Co^{2+}/Cu^{2+}. This showed that the nitrogen atom of imine group was involved in the binding with Co^{2+}/Cu^{2+}. Furthermore, ^1H NMR spectra obtained were able

Fig. 10. Color change of sensor **1** (5 mM) filter paper test strips with the increasing concentration of Co^{2+}/Cu^{2+} in 100% aqueous solution (water). (top = Co^{2+}, bottom = Cu^{2+}).

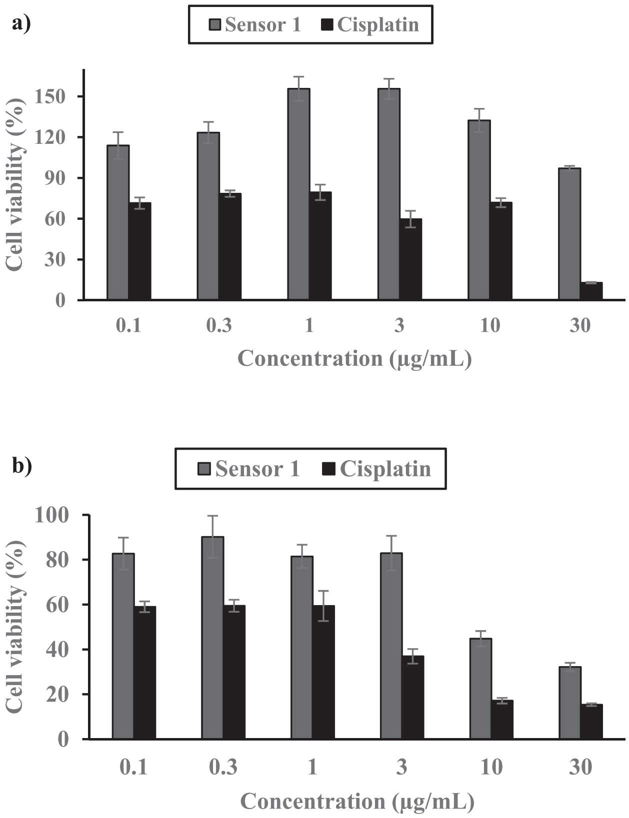

Fig. 11. Cytotoxic activity of sensor **1** against a) CCD-18Co and b) HT-29 cell lines. Cisplatin was used as positive control. Data is expressed as mean ± SD (n = 3).

to explain the binding stoichiometry of sensor **1** with Co^{2+}/Cu^{2+}. Three singlet peaks at 8.93 ppm, 9.63 ppm and 10.60 ppm were assigned to the proton of three hydroxyl group in sensor **1**. When Co^{2+} was added to sensor **1** only one of the –OH peak (9.63 ppm) showed broadening effect, indicating that only one –OH group was involved in the complexation with Co^{2+}. However when Cu^{2+} was added to sensor **1**, all three –OH peaks were broadened and started to disappear. This shows that all the –OH groups were involved in the complexation with Cu^{2+}.

ESI-MS analysis was employed to further confirm the different binding stoichiometry of sensor **1** with Co^{2+}/Cu^{2+}. As shown in Fig. S10, ESI-MS spectra of **1**-Co^{2+} and **1**-Cu^{2+} display peaks at *m*/*z* 621.21 and 443.10, which correspond to [**1** – H + Co – C_2H_5]$^+$ and 1/2[**1** – 3H + 2Cu + 2Cl + 2MeCN + H_2O]$^+$ respectively. This proves the 1:1 complexation of **1**-Co^{2+} complex and 1:2 complexation of **1**-Cu^{2+} complex.

According to the results obtained above, a proposed binding mechanism of **1** with Co^{2+}/Cu^{2+} was shown in Scheme 2. For **1**-Co^{2+}, oxygen on the amide carbonyl group, nitrogen on the imine moiety and oxygen on one of the hydroxyl group can participate in the coordination with Co^{2+}, forming a 1:1 metal complex. For **1**-Cu^{2+}, one of the Cu^{2+} binds to **1** in similar method as **1**-Co^{2+} while the other Cu^{2+} binds to the two remaining OH group, forming a 1:2 metal complex. Complexation of **1** with Co^{2+}/Cu^{2+} induced the opening of spirolactam ring, which causes the colour change from colourless to pink. For **1**-Cu^{2+}, this process is reversible as proven by the test using EDTA.

3.7. Density functional theory (DFT) calculations

To further study the interaction of sensor **1** with Co^{2+}/Cu^{2+}, Gaussian 09 program was used to carry out density functional theory (DFT) calculation [39]. Calculation was done to obtained the optimized structure of sensor **1**, **1**-Co^{2+} and **1**-Cu^{2+} at B3LYP [40–42] level using LANL2DZ basis set. Molecular orbital diagrams and HOMO-LUMO energy were also calculated at the same level of theory. As shown in Fig. 8, HOMO is distributed over the whole molecule, while LUMO is located on substituted spirolactam ring for free sensor **1**. In **1**-Co^{2+} complex, the π electrons of HOMO are mainly located on spirolocatam moiety while electrons of LUMO are mainly located on xanthene moiety. Whereas in **1**-Cu^{2+} complex, the π electrons of HOMO are mainly located on spirolactam moiety and electrons of LUMO are located in substituted ring structure. The results support the breakdown of C-N bond and opening of spirolactam ring in the complexation process to aid the reaction between the carbonyl oxygen atom and Co^{2+}/Cu^{2+}. Other than that, energy gap between HOMO and LUMO for free sensor **1**, **1**-Co^{2+}, **1**-Cu^{2+} were calculated to be 2.32739 eV, 0.60518 eV and 2.08167 eV, respectively. The reduction in the energy gap implies that metal complexes formed are more stable than free sensor **1**. Thus, the proposed coordination complexation was favourable. Furthermore, the binding stoichiometry (1:1 for **1**-Co^{2+} and 1:2 for **1**-Cu^{2+}) from DFT calculations support and complementary the results obtained from previous Job's plot, IR, ^{1}H NMR and MS studies.

3.8. Filter paper test strip application

Sensor test strips were fabricated by immersing Whatman filter paper into acetonitrile solution of sensor **1** (5 mM) for 5 min and the test strips were air-dried before use. As shown in Fig. 9, when the test strip was dipped into pure aqueous solution of Co^{2+}/Cu^{2+}, the colour of the test strip changed from colourless to pink, while other potential competitive metal ions did not produce any colour changes on the test strip. As seen from Fig. 10, increasing concen-

Table 1
Important aspects of sensor **1** and reported Co^{2+}/Cu^{2+} sensors.

Structure	Reaction condition	Target analyte	LOD (μM)	K_a (M^{-1})	Anti-interference	Rev.	Test strip	Ref.
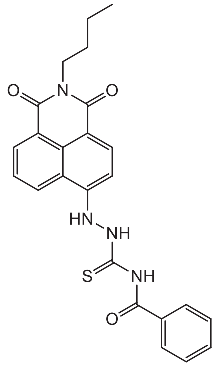	CH_3CN/HEPES (4:1, v/v, pH 7.4)	Co^{2+}	0.260	1.20 × 10^4	Good		×	[47]
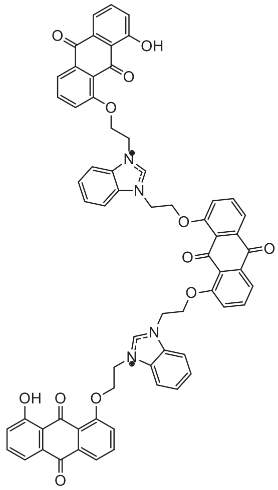	CH_3CN	Co^{2+}	0.098	1.50 × 10^5	Good	✓	×	[48]
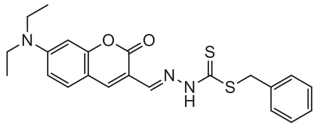	CH_3CN/HEPES (1:1, v/v, pH 7.4)	Co^{2+}	0.310	6.91 M^{-2} (log K_a)	Good	–	×	[49]
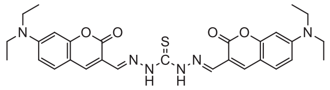	CH_3CN/HEPES (4:6, v/v, pH 7.2)	Co^{2+}	1.000	7.95 M^{-2} (log K_a)	General (Ag^+)	–	✓	[50]
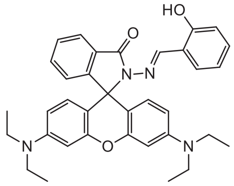	CH_3CN/Tris-HCl (5:5, v/v, pH 7.0)	Cu^{2+}	–	6.91 × 10^4	General (Fe^{2+})	✓	×	[51]
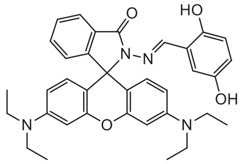	MeOH/H_2O (5:5, v/v)	Cu^{2+} Al^{3+} Fe^{3+}	0.009 0.011 0.019	1.10 × 10^6 5.90 × 10^4 5.00 × 10^4	Good Good Poor (Al^{3+}, Cu^{2+}, Cr^{3+})	– ✓ –	✓ ✓ ✓	[46]
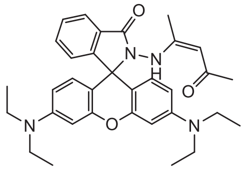	EtOH/HEPES (9:1, v/v, pH 7.0)	Cu^{2+}	2.000	6.01 × 10^4	Good	✓	×	[52]

(*continued on next page*)

Table 1 (*continued*)

Structure	Reaction condition	Target analyte	LOD (μM)	K_a (M^{-1})	Anti-interference	Rev.	Test strip	Ref.
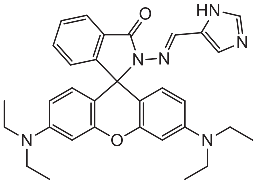	DMF/Acetate buffer (3:2, v/v, pH 3.6)	Cu^{2+}	6.470	5.72×10^4	General (Hg^{2+})	✓	×	[53]
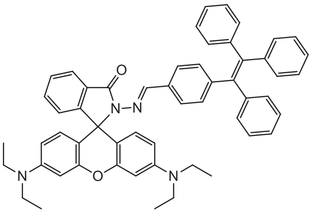	EtOH/Tris-HCl (9:1, v/v, pH 7.4)	Cu^{2+} Fe^{3+}	–	–	General (Mn^{2+}, Fe^{2+}) Poor (Co^{2+}, Cu^{2+}, Zn^{2+})	✓ ✓	×	[54]
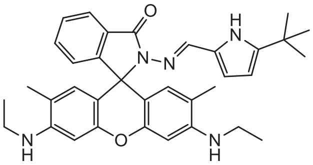	CH_3CN/H_2O (1:1, v/v)	Cu^{2+}	0.380	–	Good	×	×	[55]
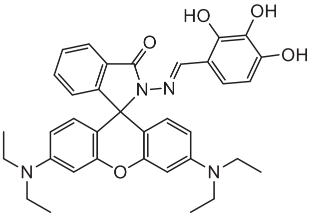	MeCN/HEPES (7:3, v/v, pH 7.0) DMF/HEPES (7:3, v/v, pH 7.0)	Co^{2+} Cu^{2+}	0.044 0.140	6.46×10^3 1.88×10^3	Good Good	× ✓	✓ ✓	This work

LOD = Limit of Detection, K_a = Association constant, Ref. = Reference.

tration of metal ions produced more intense pink colour and the test strip was able to detect Co^{2+}/Cu^{2+} as low as 5 μM. Ability of the test strip to detect low concentration metal ions in pure aqueous solution makes it useful for practical application.

3.9. Cytotoxicity of sensor **1** towards CCD-18Co and HT-29 cell lines

Selective quantification and qualification of certain species is an interesting area of current research, and bio-imaging methodology has been commonly used in analysis for metal ions. For practical bio-applicability, it is important to evaluate the cytotoxicity of the sensor in human cells. On the other hand, targeted cancer cell imaging is highly recognized owing to the support of cancer diagnose and proper treatment options. MTT assay was conducted here to study the viability of CCD-18Co and HT-29 cells after treating with sensor **1**, using cisplatin as positive control. As shown in Fig. 11, cell viability of CCD-18Co was higher than 97% after treated to a dose of 30 μg/mL (~50 μM) sensor **1** for 72 h. While for HT-29, cell viability was higher than 80% after exposure to a concentration of 3 μg/mL (~5 μM) sensor **1** for 72 h. Such results suggested that sensor **1** showed no significant cytotoxicity under the optimized condition for detection of Co^{2+}/Cu^{2+} (sensor **1** concentration: 5 μM; incubation time: <10 min), which summarize the safe use for future bio-imaging application.

3.10. Sensor **1** vs. referenced sensors

Several important aspects of sensor **1** and other reported sensors in literature studies were listed and compared in Table 1. Compared to these sensors, sensor **1** shows several good properties such as easy-to-synthesis structure, rapid response that allows real-time monitoring, wide-working pH range, low limit of detection, excellent selectivity towards targeted metal ions, reusability of sensor and ability to detect metal ions in 100% aqueous medium using fabricated test strip. Among reported Co^{2+}/Cu^{2+} sensors, most of them were single metal ion detector. For those that were multiple ion detectors, their selectivity towards target analyte will be affected by interference of other target analytes as shown in Table 1.

To the best of our knowledge, there are three rhodamine B based chemosensor with poly-hydroxybenzaldehyde moiety had been published [43–46], where all three sensors contain dihydroxybenzaldehyde moiety (2,3-, 2,4- and 2,5-). Limited hydroxyl group rendered them only the ability to target one analyte which is Cu^{2+} for 2,4-dihydroxybenzaldehyde [43] and 2,5-dihydroxybenzaldehyde [44]; Al^{3+} for 2,3-dihydroxybenzaldehyde [45]. Gupta's group was able to prepare a rhodamine B sensor with 2,5-dihydroxybenzaldehyde that can detect more than one metal ions (Cu^{2+}, Al^{3+}, Fe^{3+}) in aqueous MeOH solution. However, selectivity of sensor towards Fe^{3+} was affected in the presence of Cu^{2+} and Al^{3+} [46]. In this work, "solvent dependent sensing" method was utilized thus enabling sensor **1** to selectively detects Co^{2+}/Cu^{2+} without interfering each other in different solvent system (MeCN and DMF). Compared to reported dihydroxybenzaldehyde sensors, sensor **1** with trihydroxybenzaldehyde moiety was expected to have better water solubility due to the extra hydroxyl group that can form more hydrogen bond. Furthermore, extra hydroxyl group in the sensor allowed more possibilities of binding stoichiometry between sensor and metal ions (1:1 or 1:2), thus enabling multiple ions detection.

4. Conclusion

In conclusion, a new rhodamine B Schiff base chemosensor **1** was synthesized for the detection of Co^{2+}/Cu^{2+} in different solvent system. Real time monitoring of Co^{2+}/Cu^{2+} can be achieved by the rapid response and distinct colour change of colourless to pink. Besides, sensor **1** was showing good anti-interference properties by able to selectively detect Co^{2+}/Cu^{2+} among wide range of different metal ions. It can detect Co^{2+}/Cu^{2+} with high sensitivity, while exhibiting low detection limit of 4.425×10^{-8} M and 1.398×10^{-7} M respectively. Other than that, a low cost chemosensor test strips were fabricated for the convenient "naked-eye" detection of Co^{2+} and Cu^{2+} in pure aqueous media. Furthermore, no notable cytotoxicity of sensor **1** in CCD-18Co and HT-29 cell lines showing its potential to be used in bio-imaging application.

CRediT authorship contribution statement

Wei Chuen Chan: Writing - original draft, Validation, Investigation, Visualization, Data curation, Methodology, Conceptualization. **Hazwani Mat Saad:** Validation, Investigation. **Kae Shin Sim:** Writing - review & editing, Supervision. **Vannajan Sanghiran Lee:** Writing - review & editing, Supervision. **Chee Wei Ang:** Validation, Investigation. **Keng Yoon Yeong:** Validation, Investigation. **Kong Wai Tan:** Writing - review & editing, Supervision.

Declaration of Competing Interest

The authors declare that they have no known competing financial interests or personal relationships that could have appeared to influence the work reported in this paper.

Acknowledgement

The authors are thankful to MOHE, Malaysia (FGRS/1/2019/STG01/UM/02/11) for funding.

Appendix A. Supplementary data

Supplementary data to this article can be found online at https://doi.org/10.1016/j.saa.2021.120099.

References

[1] L. Prashanth, K. Kattapagari, R. Chitturi, V. Baddam, L. Prasad, A review on role of essential trace elements in health and disease, J. Dr. NTR Univ. Health Sci. 4 (2) (2015) 75–85.

[2] A. Mirza, A. King, C. Troakes, C. Exley, Aluminium in brain tissue in familial Alzheimer's disease, J. Trace Elem. Med. Biol. 40 (2017) 30–36.

[3] S. Okamoto, L.D. Eltis, The biological occurrence and trafficking of cobalt, Metallomics 3 (10) (2011) 963–970.

[4] C. Little, S.E. Aakre, M.G. Rumsby, K. Gwarsha, Effect of Co2+-substitution on the substrate specificity of phospholipase C from Bacillus cereus during attack on two membrane systems, Biochem. J. 207 (1) (1982) 117–121.

[5] D. Lindsay, W. Kerr, Cobalt close-up, Nat. Chem. 3 (6) (2011) 494.

[6] M. Dennis, P.E. Kolattukudy, A cobalt-porphyrin enzyme converts a fatty aldehyde to a hydrocarbon and CO, Proc. Natl. Acad. Sci. U.S.A. 89 (12) (1992) 5306.

[7] K. Jomova, M. Valko, Advances in metal-induced oxidative stress and human disease, Toxicology 283 (2) (2011) 65–87.

[8] E.L. Que, D.W. Domaille, C.J. Chang, Metals in neurobiology: probing their chemistry and biology with molecular imaging, Chem. Rev. 108 (5) (2008) 1517–1549.

[9] J.C. Lee, H.B. Gray, J.R. Winkler, Copper(II) binding to alpha-synuclein, the Parkinson's protein, J Am Chem Soc 130 (22) (2008) 6898–6899.

[10] S. Bagheri, R. Squitti, T. Haertlé, M. Siotto, A.A. Saboury, Role of copper in the onset of Alzheimer's disease compared to other metals, Front. Aging Neurosci. 9 (2018) 446.

[11] C. Vulpe, B. Levinson, S. Whitney, S. Packman, J. Gitschier, Isolation of a candidate gene for Menkes disease and evidence that it encodes a copper–transporting ATPase, Nat. Genet. 3 (1) (1993) 7–13.

[12] E. Madsen, J.D. Gitlin, Copper and Iron Disorders of the Brain, Annu. Rev. Neurosci. 30 (1) (2007) 317–337.

[13] L.M. Gaetke, C.K. Chow, Copper toxicity, oxidative stress, and antioxidant nutrients, Toxicology 189 (1) (2003) 147–163.

[14] A.P.S. Gonzáles, M.A. Firmino, C.S. Nomura, F.R.P. Rocha, P.V. Oliveira, I. Gaubeur, Peat as a natural solid-phase for copper preconcentration and determination in a multicommuted flow system coupled to flame atomic absorption spectrometry, Anal. Chim. Acta 636 (2) (2009) 198–204.

[15] Y. Liu, P. Liang, L. Guo, Nanometer titanium dioxide immobilized on silica gel as sorbent for preconcentration of metal ions prior to their determination by inductively coupled plasma atomic emission spectrometry, Talanta 68 (1) (2005) 25–30.

[16] Y. Gao, W. Ma, Study on a colorimetric sensor with color switching: Naked-eye detection for Cu(II) ion, Opt. Mater. 35 (2) (2012) 211–216.

[17] S. Mohandoss, T. Stalin, A new fluorescent PET sensor probe for Co2+ ion detection: computational, logic device and living cell imaging applications, RSC Adv. 7 (27) (2017) 16581–16593.

[18] W. He, Z. Liu, A fluorescent sensor for Cu2+ and Fe3+ based on multiple mechanisms, RSC Adv. 6 (64) (2016) 59073–59080.

[19] Y. Fu, Q.-C. Feng, X.-J. Jiang, H. Xu, M. Li, S.-Q. Zang, New fluorescent sensor for Cu2+ and S2– in 100% aqueous solution based on displacement approach, Dalton Trans. 43 (15) (2014) 5815–5822.

[20] Y.N. Choi, I.W. Park, S.S. Kim, S.S. Park, S.H. Choh, Electron paramagnetic resonance studies of Co2+ions in congruent and nearly stoichiometric LiNbO3single crystals, J. Condens. Matter Phys. 11 (24) (1999) 4723–4730.

[21] A.B. Vassilikou-Dova, K. Eftaxias, Electron paramagnetic resonance of Cu2+in descloizite mineral: an unusual electronic configuration, J. Condens. Matter Phys. 4 (1) (1992) 241–248.

[22] J.-R. Zhou, D.-P. Liu, Y. He, X.-J. Kong, Z.-M. Zhang, Y.-P. Ren, L.-S. Long, R.-B. Huang, L.-S. Zheng, A highly selective colorimetric chemosensor for cobalt(ii) ions based on a tripodal amide ligand, Dalton Trans. 43 (30) (2014) 11579–11586.

[23] S. Mukhopadhyay, R.K. Gupta, A. Biswas, A. Kumar, M. Dubey, M.S. Hundal, D.S. Pandey, A dual-responsive "turn-on" bifunctional receptor: a chemosensor for Fe3+ and chemodosimeter for Hg2+, Dalton Trans. 44 (16) (2015) 7118–7122.

[24] Y. Gao, C. Zhang, S. Peng, H. Chen, A fluorescent and colorimetric probe enables simultaneous differential detection of Hg2+ and Cu2+ by two different mechanisms, Sens. Actuators B Chem. 238 (2017) 455–461.

[25] M. Chhatwal, A. Kumar, V. Singh, R.D. Gupta, S.K. Awasthi, Addressing of multiple-metal ions on a single platform, Coord. Chem. Rev. 292 (2015) 30–55.

[26] P.W. Cheah, M.P. Heng, A. Izati, C.H. Ng, K.W. Tan, Rhodamine B conjugate for rapid colorimetric and fluorimetric detection of aluminium and tin ions and its application in aqueous media, Inorganica Chim. Acta 512 (2020) 119901.

[27] Y. Wang, Z.-G. Wang, X.-Q. Song, Q. Chen, H. Tian, C.-Z. Xie, Q.-Z. Li, J.-Y. Xu, A dual functional turn-on non-toxic chemosensor for highly selective and sensitive visual detection of Mg2+ and Zn2+: the solvent-controlled recognition effect and bio-imaging application, Analyst 144 (13) (2019) 4024–4032.

[28] L. Fan, J.-C. Qin, T.-R. Li, B.-D. Wang, Z.-Y. Yang, A novel rhodamine chromone-based "Off–On" chemosensor for the differential detection of Al(III) and Zn(II) in aqueous solutions, Sens. Actuators B Chem. 203 (2014) 550–556.

[29] Agilent, CrysAlis PRO, p. Agilent Technologies Ltd, Yarnton, Oxfordshire, England, 2014.

[30] G. Sheldrick, A short history of SHELX, Acta Crystallogr., Sect. A 64 (1) (2008) 112–122.

[31] O.V. Dolomanov, L.J. Bourhis, R.J. Gildea, J.A.K. Howard, H. Puschmann, OLEX2: a complete structure solution, refinement and analysis program, J. Appl. Crystallogr. 42 (2) (2009) 339–341.

[32] C.F. Macrae, P.R. Edgington, P. McCabe, E. Pidcock, G.P. Shields, R. Taylor, M. Towler, J. van de Streek, Mercury: visualization and analysis of crystal structures, J. Appl. Crystallogr. 39 (3) (2006) 453–457.

[33] L.J. Farrugia, ORTEP-3 for Windows - a version of ORTEP-III with a Graphical User Interface (GUI), J. Appl. Crystallogr. 30 (5-1) (1997) 565.

[34] M.P. Heng, C.H. Tan, H.M. Saad, K.S. Sim, K.W. Tan, Mitochondria-dependent apoptosis inducer: Testosterone-N4-ethylthiosemicarbazonate and its metal complexes with selective cytotoxicity towards human colorectal carcinoma cell line (HCT 116), Inorganica Chim. Acta 507 (2020) 119581.

[35] M. Kumar, A. Kumar, M.K. Singh, S.K. Sahu, R.P. John, A novel benzidine based Schiff base "turn-on" fluorescent chemosensor for selective recognition of Zn2+, Sens. Actuators B Chem. 241 (2017) 1218–1223.

[36] E. Zhang, P. Ju, Q. Li, X. Hou, H. Yang, X. Yang, Y. Zou, Y. Zhang, A novel rhodamine 6G-based fluorescent and colorimetric probe for Bi3+: synthesis, selectivity, sensitivity and potential applications, Sens. Actuators B Chem. 260 (2018) 204–212.

[37] M. Tian, H. He, B.-B. Wang, X. Wang, Y. Liu, F.-L. Jiang, A reaction-based turn-on fluorescent sensor for the detection of Cu (II) with excellent sensitivity and selectivity: Synthesis, DFT calculations, kinetics and application in real water samples, Dyes Pigm. 165 (2019) 383–390.

[38] T. Ackermann, K.A. Connors, Binding constants — the measurement of molecular complex stability, John Wiley & Sons, New York, Chichester, Brisbane, Toronto, Singapore 1987. 411 Seiten, Preis: £ 64.15. Berichte der Bunsengesellschaft für physikalische Chemie, 1987. 91(12): p. 1398-1398.

[39] M. Frisch, G. Trucks, H. Schlegel, G. Scuseria, M. Robb, J. Cheeseman, G. Scalmani, V. Barone, B. Mennucci, G. Petersson, H. Nakatsuji, M. Caricato, X. Li, H. Hratchian, A. Izmaylov, J. Bloino, G. Zheng, J. Sonnenberg, M. Hada, D. Fox, Gaussian 09 (Revision A02), Gaussian Inc., Wallingford CT, 2009.

[40] A.D. Becke, Density-functional thermochemistry. III. The role of exact exchange, J. Chem. Phys. 98 (7) (1993) 5648–5652.

[41] C. Lee, W. Yang, R.G. Parr, Development of the Colle-Salvetti correlation-energy formula into a functional of the electron density, Phys. Rev. B 37 (2) (1988) 785–789.

[42] B. Miehlich, A. Savin, H. Stoll, H. Preuss, Results obtained with the correlation energy density functionals of becke and Lee, Yang and Parr, Chem. Phys. Lett. 157 (3) (1989) 200–206.

[43] Z. Xu, L. Zhang, R. Guo, T. Xiang, C. Wu, Z. Zheng, F. Yang, A highly sensitive and selective colorimetric and off–on fluorescent chemosensor for Cu2+ based on rhodamine B derivative, Sens. Actuators B Chem. 156 (2) (2011) 546–552.

[44] P. Milindanuth, P. Pisitsak, A novel colorimetric sensor based on rhodamine-B derivative and bacterial cellulose for the detection of Cu(II) ions in water, Mater. Chem. Phys. 216 (2018) 325–331.

[45] A. Dhara, A. Jana, N. Guchhait, P. Ghosh, S.K. Kar, Rhodamine-based molecular clips for highly selective recognition of Al3+ ions: synthesis, crystal structure and spectroscopic properties, New J. Chem. 38 (4) (2014) 1627–1634.

[46] V.K. Gupta, N. Mergu, L.K. Kumawat, A new multifunctional rhodamine-derived probe for colorimetric sensing of Cu(II) and Al(III) and fluorometric sensing of Fe(III) in aqueous media, Sens. Actuators B Chem. 223 (2016) 101–113.

[47] Y.L. Liu, L. Yang, L. Li, Y.Q. Guo, X.X. Pang, P. Li, F. Ye, Y. Fu, A New Fluorescent Chemosensor for Cobalt(II) Ions in Living Cells Based on 1,8-Naphthalimide, Molecules 24 (17) (2019).

[48] Q.-X. Liu, Z.-L. Hu, Z.-X. Zhao, A new fluorescent–colorimetric chemosensor for cobalt(ii) ions based on bis-benzimidazolium salt with three anthraquinone groups, New J. Chem. 42 (24) (2018) 20049–20055.

[49] Z. Liu, W. Wang, H. Xu, L. Sheng, S. Chen, D. Huang, F. Sun, A "naked eye" and ratiometric chemosensor for cobalt(II) based on coumarin platform in aqueous solution, Inorg. Chem. Commun. 62 (2015) 19–23.

[50] D. Maity, T. Govindaraju, Highly selective colorimetric chemosensor for Co2+, Inorg. Chem. 50 (22) (2011) 11282–11284.

[51] Y. Xiang, A. Tong, P. Jin, Y. Ju, New fluorescent rhodamine hydrazone chemosensor for Cu(II) with high selectivity and sensitivity, Org. Lett. 8 (13) (2006) 2863–2866.

[52] Y. Hu, J. Zhang, Y.-Z. Lv, X.-H. Huang, S.-L. Hu, A new rhodamine-based colorimetric chemosensor for naked-eye detection of Cu(2+) in aqueous solution, Spectrochim. Acta A Mol. Biomol. Spectrosc. 157 (2016) 164–169.

[53] J. Ding, L. Yuan, L. Gao, J. Chen, Fluorescence quenching of a rhodamine derivative: Selectively sensing Cu2+ in acidic aqueous media, J. Lumin. 132 (8) (2012) 1987–1993.

[54] Y. Yang, C.-Y. Gao, N. Zhang, D. Dong, Tetraphenylethene functionalized rhodamine chemosensor for Fe3+ and Cu2+ ions in aqueous media, Sens. Actuators B Chem. 222 (2016) 741–746.

[55] Z. Guo, X. Wang, P. Wei, Y. Gao, Q. Li, Highly selective fluorescent probe for the detection of copper (II) and its application in live cell imaging, J. Anal. Methods Chem. 2019 (2019) 8130767.